

Nanometerizing Taxifolin Into Selenized Liposomes to Ameliorate Its Hypoglycemic Effect by Optimizing Drug Release and Bioavailability

Chunli Qi^{1-3,*}, Huijie Xing^{2,3,*}, Ning Ding⁴, Weifeng Feng⁵, Yongyi Wu⁶, Xingwang Zhang⁷, Yigang Yu¹

¹School of Food Science and Engineering, South China University of Technology, Guangzhou, 510641, People's Republic of China; ²Institute of Laboratory Animals, Jinan University, Guangzhou, 510632, People's Republic of China; ³Key Laboratory of Viral Pathogenesis & Infection Prevention and Control (Jinan University), Ministry of Education, Guangzhou, 510632, People's Republic of China; ⁴Department of Animal, Plant and Food, Guangzhou Customs Technology Center, Guangzhou, 510623, People's Republic of China; ⁵Department of Traditional Chinese Medicine, The First Affiliated Hospital of Jinan University, Guangzhou, 510630, People's Republic of China; ⁶Zhongshan School of Medicine, Sun Yat-Sen University, Guangzhou, 510080, People's Republic of China; ⁷Department of Pharmaceutics, School of Pharmacy, Jinan University, Guangzhou, 511443, People's Republic of China

*These authors contributed equally to this work

Correspondence: Xingwang Zhang, Email zhangxw@jnu.edu.cn; Yigang Yu, Email yuyigang@scut.edu.cn

Purpose: Diabetes mellitus (DM) remains a significant health challenge, with traditional treatments often failing to provide lasting solutions. Taxifolin (Tax), a potential phytochemistry with antioxidant and anti-hyperglycemic properties, suffers from low water solubility and poor bioavailability, necessitating advanced delivery systems. This study aims to nanometerize taxifolin (Tax) into selenized liposomes (Tax-Se@LPs) for enhanced oral delivery and hypoglycemic effect.

Methods: Tax-Se@LPs were fabricated through a thin-film hydration/in situ reduction technique. The resulting nanomedicine was characterized through in vitro release studies, pharmacokinetic and pharmacodynamic evaluations, cellular uptake assays, and formulation stability tests.

Results: The optimized Tax-Se@LPs demonstrated an average particle size of 185.3 nm and an entrapment efficiency of 95.25% after optimization. In vitro release studies revealed that Tax-Se@LPs exhibited a slower and more sustained release profile compared to conventional liposomes, favoring gastrointestinal drug absorption. Pharmacokinetic evaluations in normal rats indicated that Tax-Se@LPs achieved a relative bioavailability of 216.65%, significantly higher than Tax suspensions and unmodified liposomes. Furthermore, in diabetic GK rats, Tax-Se@LPs resulted in a maximal blood glucose reduction of 46.8% and exhibited a more sustained therapeutic duration compared to other formulations. Cellular uptake tests manifested that selenization altered the internalization mechanisms of liposomes while preserving their absorption aptness by intestinal epithelial cells. The physiological and in vitro stability of Tax-Se@LPs was also reinforced by selenization.

Conclusion: Overall, Tax-Se@LPs not only improve the oral bioavailability of Tax but also enhance its therapeutic efficacy. These findings underscore the potential of Tax-Se@LPs as a promising therapeutic strategy for DM management.

Keywords: taxifolin, liposomes, selenium, diabetes mellitus, bioavailability, hypoglycemic effect

Introduction

Diabetes mellitus (DM) is a chronic metabolic disease characterized by high incidence and significant health risks that currently cannot be cured.¹ According to the latest available data (2020–2024) from International Diabetes Federation (IDF), the global prevalence of DM continues to escalate, reaching approximately 10.5% among adults aged 20–79 years in 2023. Traditional treatments, such as oral hypoglycemic drugs and insulin injection, can merely alleviate symptoms and slow disease progression, failing to reverse tissue and organ damage or prevent complications. These treatments may also lead to potential side effects and adverse reactions.² Phytochemicals exhibit multifaceted treatment against diabetes with fewer untoward

effects, presenting new hope for managing this disorder, especially with advances in drug delivery technology.^{3,4} Emerging evidence demonstrates that phytochemicals-laden nanomedicines are promising for DM management.⁵

Taxifolin (Tax), also known as dihydroquercetin (Figure 1), is a member of the vitamin P family. This prominent phytomedicine is naturally derived from various plant sources, eg, Siberian larch (*Larix sibirica*), French maritime pine (*Pinus pinaster*), and onions (*Allium cepa*). Renowned for its potent biological activities and therapeutic potential, Tax has garnered considerable attention for its role in managing chronic diseases. Its superior structure grants Tax strong antioxidant properties,⁶ earning it the title of “King of free radicals scavenging”. Numerous studies have demonstrated that Tax exhibits excellent anti-inflammatory, anti-cancer, anti-dementia, anti-radiation, and hepatoprotective/cardiovascular protective properties.⁷ In addition, Tax demonstrates significant anti-hyperglycemic activities across various diabetic models,^{8,9} able to enhance insulin sensitivity, improves glucose uptake, and modulates glucose metabolism, making it a promising candidate for diabetes management. However, its low water solubility and limited bioavailability pose large challenges for practical application. Thus, there is a strong interest in developing advanced oral delivery systems for Tax to address these issues.

Lipid-based formulations can significantly promote the absorption of lipophilic and poorly permeable compounds.¹⁰ Various lipid-based formulations, such as lipid nanoparticles (SLN and NLC),¹¹ liposomes,¹² emulsions,¹³ biomimetic nanovesicles,¹⁴ and exosomes,¹⁵ have been explored for the oral delivery of challenging drugs. Among them, liposomes stand out as effective nanocarriers that can improve drug absorption and therapy. However, their structural defects often lead to variable absorption profiles during digestion.¹⁶ To this end, several stabilization strategies have been proposed for structural optimization of liposomes, including PEGylation,^{17,18} mineralization,^{19,20} coating with polymers,^{21,22} and surface engineering with biomaterials.^{23,24} Mineralizing the lipid bilayer safeguards liposomes from gastrointestinal digestive degradation and facilitates payload delivery via intact nanovesicles, making it an effective approach for optimizing liposomal structure and drug delivery. Depositing selenium on liposomes through in situ reduction can be regarded as a form of mineralization process. The remarkable stability of the selenium layer on liposomes in the gastrointestinal environment significantly enhances the overall stability of the liposomal system. While a number of selenium-functionalized nanocarriers have been reported to ameliorate drug delivery and therapy,^{25–29} selenized liposomes have yet to be explored for the oral delivery of Tax for hypoglycemic purposes.

In this study, selenized liposomes (Se@LPs) were developed for the oral delivery of Tax to investigate their hypoglycemic effect in diabetic models. Tax-loaded Se@LPs (Tax-Se@LPs) were fabricated by a thin-film hydration/ in situ reduction technique and characterized through various formulation indices, drug release, and in vitro/vivo stability. The oral bioavailability and hypoglycemic effect were evaluated in normal and diabetic rats, while the mechanisms behind ameliorative absorption and therapeutic efficacy were explored through cell tests.

Materials and Methods

Materials

Taxifolin was purchased from Macklin Biochemical Co., Ltd. (Shanghai, China). Soybean lecithin with phosphatidylcholine over 90% was procured from Alfa Aesar Chemicals Co. Ltd. (Shanghai, China). Cholesterol, Hoechst 33258 and lipase from the porcine pancreas (>3000 IU/g) were provided by Sinopharm Chemical Reagent Co., Ltd (Shanghai,

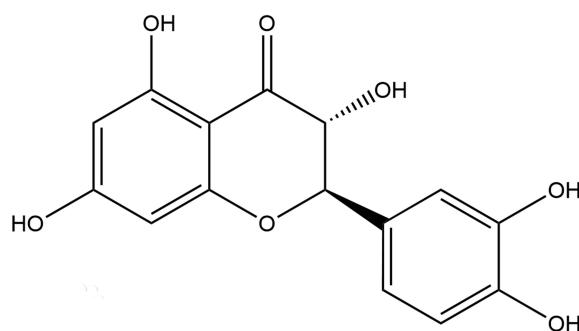


Figure 1 Chemical structure of taxifolin.

China). Simulated gastric fluid (SGF) containing pepsin and simulated intestinal fluid (SIF) containing trypsin were purchased from Coolaber (Beijing, China). Sodium selenite (Na_2SeO_3) and reduced glutathione (r-GSH) were obtained from Aladdin Reagent (Shanghai, China). DiO (3,3'-dioctadecyloxacarbocyanine perchlorate) was from Quansu Biotech Co., Ltd. (Beijing, China). Deionized water used was the product of Wahaha Group (Hangzhou, China). All other chemicals were of analytical grade and used as received.

Preparation of Tax-Se@LPs

Tax-Se@LPs were prepared by the thin-film hydration/in situ reduction technique.²⁰ Briefly, lecithin, cholesterol, and Tax were dissolved in a flask with anhydrous ethanol. Afterward, anhydrous ethanol was removed by evaporation under a reduced pressure at 35°C. The resulting thin lipid film was then hydrated at 55°C against a Na_2SeO_3 solution (1 mg/mL). After complete hydration, quadruple moles of GSH to Na_2SeO_3 were introduced to trigger the reduction reaction. The system was maintained at 37°C under agitation at 1,000 rpm. Tax-Se@LPs were obtained upon reaction for 2 h. The reference preparation of Tax-LPs followed the same procedure of Tax-Se@LPs except the addition of r-GSH. In addition, DiO-labeled Tax-LPs and Tax-Se@LPs were fabricated for cell test in the same way.

Characterization of Tax-Se@LPs

Tax-Se@LPs were characterized through particle size, ζ potential, morphology, and entrapment efficacy (*EE*). All tests were performed in triplicate in parallel with Tax-LPs as a reference. The particle size and ζ potential of Tax-Se@LPs were measured by a particle size/potential analyzer (Zetasizer Nano ZS, Malvern, Worcestershire, UK) after appropriate dilution with deionized water.³⁰ The samples were equilibrated for 120 s at 25°C and then subjected to laser diffraction or Doppler velocimetry, respectively, for the output of particle size and ζ potential.

The morphology of Tax-Se@LPs was visualized with a transmission electron microscopy (TEM, Libra 120, Zeiss, Oberkochen, Germany). An aliquot of Tax-Se@LPs, diluted by 25 folds with water, was fixed on a carbon-coated copper grid by dehydration under a warm light lamp. The fixed lipid vesicles were then observed by TEM where typical photographs were taken at an acceleration voltage of 100 kV.

The *EE* of Tax-Se@LPs was measured by a reported centrifugal ultrafiltration technique.²⁷ Briefly, an appropriate amount of Tax-Se@LPs was first centrifuged at 5,000 rpm for 5 min to remove unwrapped bulk drug. The resulting nanosuspensions were further proceeded to centrifuge against a centrifugal filter device (Amicon® Ultra-0.5, MWCO 100K, Millipore, USA) to separate free drug from the colloidal solution. The concentration of Tax encapsulated in liposomes was analyzed by UPLC established below. The *EE* was defined as the percentage of free drug (C_{fre}) to total drug (C_{tot}) and calculated according to equation (1) below:

$$EE(\%) = C_{\text{fre}} / C_{\text{tot}} \times 100\% \quad (1)$$

In vitro Release Study

The in vitro release of Tax from Tax-Se@LPs was investigated by the dialysis method using distilled water, 0.1 M HCl, and pH 6.8 phosphate buffered saline (PBS) as release media.³¹ To create a sink condition, 0.5% sodium dodecyl sulfate (SDS) was used in the media to solubilize the drug. Aliquots of Tax-LPs and Tax-Se@LPs equal to 5 mg Tax were loaded into dialysis bags and placed in 100 mL of release medium. At predetermined time points, 250 μL of sample was withdrawn from the release medium. The samples were filtered through a filter membrane and then subjected to UPLC analysis. The accumulative percentage of release was calculated to plot the release profiles.

Tax quantification was performed using an ACQUITY ULPC H-Class system consisting of a quaternary pump, an autosampler, and a PDA detector (Waters, MA, USA). The samples were separated with a Poroshell HPH-C18 column (2.6 μm , 2.1 \times 50 mm, Waters) at 35°C with injection volume of 5 μL . A mobile phase composed of methanol and 0.1% phosphoric acid solution (65/35) pumped at a flow rate of 0.2 mL/min was employed to elute the samples. The eluates were monitored at 291 nm.

Oral Bioavailability

Sprague Dawley (SD) rats were used to investigate the oral pharmacokinetics of Tax-Se@LPs and reference preparations. Fifteen 6-week-old rats weighing 220 ± 20 g were randomly divided into three groups ($n = 5$), namely Tax suspensions, Tax@LPs, and Tax-Se@LPs. Before the experiment, the rats were fasted overnight but free access to water. Upon administration, they were given the corresponding preparations by gavage at a dose of 20 mg/kg equivalent to Tax.³² Aliquots of blood (~0.25 mL) were collected into the heparinized tubes from the caudal vein at 0.5, 1, 2, 4, 6, 8, 12, 16, and 24 h after dosing. The protocols for animal study were reviewed and approved by the Experimental Animal Ethical Committee of Jinan University (Approval No: IACUC-20240913-03), and the animals were treated as per The Guide for the Care and Use of Laboratory Animals published by the National Research Council (NRC). The plasmas were prepared from the blood samples by centrifugation at 5,000 rpm for 5 min. After that, the supernatant plasmas were transferred to new centrifugal tubes ready for UPLC analysis.

To quantify the drug concentration, we utilized a protein precipitation procedure to retrieve Tax from the plasma. Briefly, 100 μ L of plasma was mixed with 500 μ L of methanol followed by a strong vortex for 3 min. The mixture was centrifuged at 8,000 rpm for 10 min to force phase separation. The supernatants were withdrawn and evaporated into free solvent using a centrifugal concentrator (Hexi, Changsha, China). The residues were reconstituted in 50 μ L of fluid phase for liquid chromatograph/mass spectrometer (LC/MS) analysis. Tax quantification utilized a quantitative curve spiked with varying levels of Tax in blank plasma, analyzed using a QTRAP® 4500 LC/MS (AB SCIEX, MA, USA).³³ Samples were eluted against a gradient of formic acid (0.1%) in water (mobile phase A) versus acetonitrile (mobile phase B) at a flow rate of 0.3 mL/min, following this program: 5% B from 0 to 4 min, increasing to 90% B from 4 to 7 min, holding at 90% B from 7 to 9 min, and returning to 5% B from 9 to 12 min. PKSolver 2.0, an add-in program for pharmacokinetic analysis, was adopted to process the data and get the pharmacokinetic parameters.

Hypoglycemic Effect

The hypoglycemic effect of Tax-Se@LPs was examined in Goto-Kakizaki (GK) diabetic rats. GK rats weighing 250 ± 20 g were randomized into five groups ($n = 5$). The rats were fasted for 12 h before the experiment but accessible to water *ad libitum*. Four groups of rats were orally given saline, Tax suspensions, Tax@LPs, and Tax-Se@LPs, respectively, with a dose of 30 mg/kg.³⁴ The rats in the positive control group were subcutaneously injected with insulin solution (1 IU/kg). After administration, approximately 250 μ L of blood was collected from the caudal vein at preset intervals and immediately centrifuged at 5,000 g for 5 min to obtain the plasma. The plasma glucose level was immediately measured using a glucose assay kit (Jiancheng Bioengineering Institute, Nanjing, China). Blood glucose concentration was calculated by equation (2) below:

$$\text{Blood glucose (mM)} = \frac{A_s - A_b}{A_c - A_b} \times 5.05 \quad (2)$$

where A_s , A_b , and A_c denote the absorbance of test sample, blank sample, and calibration sample, respectively, and 5.05 is the glucose concentration of the calibration solution.

Cell Uptake/Internalization Assay

The intestinal epithelial absorption of Tax-LPs and Tax-Se@LPs was evaluated in Caco-2 cells by flow cytometry and confocal laser scanning microscopy (CLSM) imaging. DiO-stained Tax-LPs and Tax-Se@LPs were specially prepared and used for the observation of cellular uptake and internalization. Tax-LPs and Tax-Se@LPs with fluorescence were incubated with Caco-2 cells for 1, and 2 h at 37°C at a Tax concentration of 10 μ g/mL, respectively. The cells were then washed twice with a pH 7.4 HBSS and sent to determine the uptake rate on a flow cytometry (FACSCanto, BD, NY, USA). In addition, the relative cellular uptake of Tax-Se@LPs in the presence of various transport inhibitors was examined to analyze the cellular trafficking mechanisms.³⁵

To detect the cellular internalization, Caco-2 cells were seeded in a confocal Petri dish balanced with cell culture medium previously. Cells were grown for 24 h at a density of 5×10^4 cell/mL. The DiO-labeled Tax-LPs and Tax-Se@LPs were then introduced into the wells with a confocal dish to incubate for 0.5 h. After incubation, the cells were

washed twice with cold HBSS, fixed in 4% paraformaldehyde for 1 h, and stained with Hoechst 33258. The internalized nanovesicles by Caco-2 cells were visualized through a LSM800 CLSM (Zeiss, Wetzlar, Germany).

In vitro/vivo Stability

The in vitro stability of Tax-Se@LPs was evaluated by particle size and PDI upon storing in refrigerator at 4°C and exposure to ambient conditions. The in vivo stability was checked in biorelevant media (SGF and SIF) to simulate the physiological transport process. The changes in particle size, PDI, and ζ potential of Tax-LPs and Tax-Se@LPs in simulated physiological fluids were measured as per the previously reported procedure.²⁷

Results and Discussion

Preparation and Characterization of Tax-Se@LPs

Tax-Se@LPs were prepared using a combined technique of thin-film hydration followed by ultrasonic homogenization. The formulation composition and preparation process significantly influence the physicochemical characteristics of nanovehicles. Critical parameters including particle size and PDI were found to be dependent on several key factors: the lecithin-to-cholesterol ratio, drug-to-lipid ratio, Na_2SeO_3 concentration upon selenization, and the duration of ultrasonication treatment. As demonstrated in Figure 2, these formulation variables exhibit substantial impacts on the

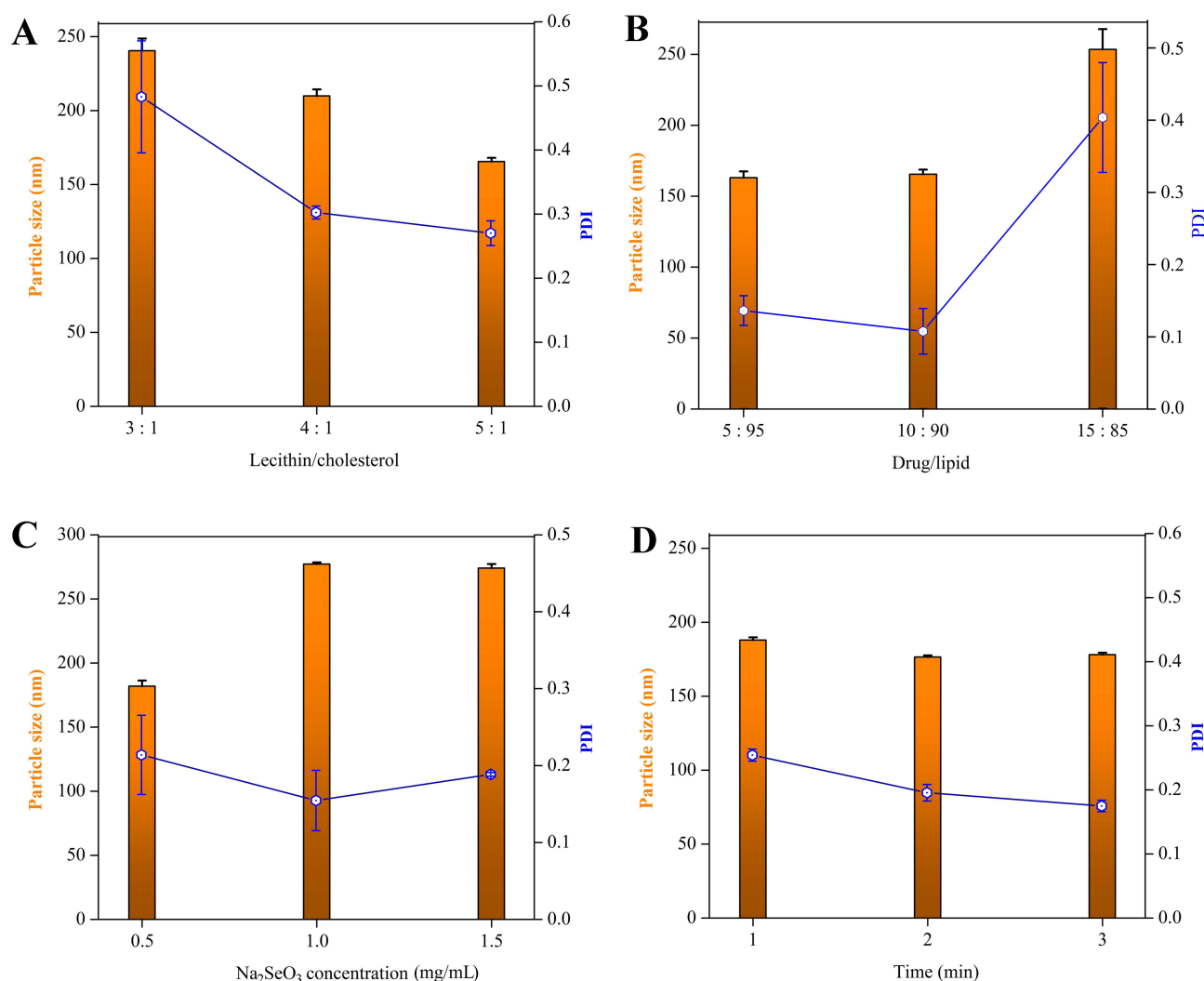


Figure 2 Variables affecting the particle size and polydispersity index (PDI) of Tax-Se@LPs, including the lecithin/cholesterol ratio (A), the drug/lipid ratio (B), Na_2SeO_3 concentration during selenization (C), and ultrasonication duration upon homogenization (D).

structural and functional properties of Tax-Se@LPs. The lecithin/cholesterol ratio significantly affected the particle size and PDI of liposomes. An optimal ratio of 5:1 produced smaller nanovesicles with reduced PDI. Higher cholesterol levels, due to a high phase-transition temperature, were unfavorable for liposome formation, while a higher drug content was also detrimental. Therefore, a drug content of 10% was ideal for liposome development. Additionally, the concentration of Na₂SeO₃ markedly influenced the particle size of Tax-Se@LPs, with significant size increases occurring at concentrations above 0.5 mg/mL, although PDI remained unchanged, indicating a concentration-dependent selenium deposition. Of note, the effect of ultrasonication time on the particle size was marginal, and a short ultrasound treatment could obtain liposomes with narrow particle size distribution. Taken together, the final formulation was composed of 75 mg of lecithin, 15 mg of cholesterol, and 10 mg of Tax, which was hydrated against 20 mL of Na₂SeO₃ solution (0.5 mg/mL) and subjected to 1 minute of ultrasonication after hydration.

Tax-Se@LPs, prepared from the screened formulation, had an average particle size of 185.3 nm and a narrow distribution (PDI = 0.213) (Figure 3A). Se-mineralized liposomes (Tax-Se@LPs) appeared purplish red, unlike the conventional liposomes (Tax-LPs) (Figure 3B). Both types of liposomes exhibited spherical morphology as presented by TEM (Figure 3C). However, a higher electron-dense corona was provided with Tax-Se@LPs, indicating Se deposition onto their surfaces.^{20,27} The ζ potential of Tax-Se@LPs was measured at -28.6 mV, reflecting good colloidal stability due to an absolute potential over 25 mv.³⁶ The *EE* of Tax-Se@LPs was up to 95.25%, attributed to the high hydrophobicity of Tax, which promotes drug supersaturation in the colloidal system for effective oral delivery.

In vitro Release

In vitro release studies can predict the *in vivo* absorption and transport behaviors of drugs and their carriers. Burst release may hinder drug absorption due to the risk of drug precipitation.³⁷ An ideal formulation should enable concurrent absorption of both free and carrier-encapsulated drugs with an optimal release profile. Figure 4 illustrates the release of Tax from Tax-LPs and Tax-Se@LPs over time across different media. Tax-Se@LPs exhibited slower release rates, with cumulative release percentages at 12 h being 46.54% in 0.1 M HCl, 55.67% in water, and 52.73% in pH 6.8 PBS. However, there was a significant difference in release between Tax-LPs and Tax-Se@LPs across all media, attributed to the deposition of Se on the liposome surface, which retarded drug release as a sustained coating.³⁸ Sustained release lowers the risk of supersaturated precipitation of burst-released free drug while promoting absorption through a carrier-mediated cotransport mechanism.³

The modality of drug in the gastrointestinal transport process significantly influences its absorption.³⁹ A small quantity of drug released from its preparation allows for immediate absorption at the absorptive epithelium, while a larger amount retained in the formulation can sustain drug release, providing a long-acting therapeutic effect. The release media of 0.1 M HCl, pH 6.8 PBS, and deionized water represent the commonly encountered conditions of drug and formulation transport after oral administration. In contrast, Tax-Se@LPs release the drug more slowly than Tax-LPs, regardless of the release medium. This attribute of drug release for Tax-Se@LPs promises ameliorable drug absorption.

Enhanced Oral Bioavailability

The pharmacokinetic profiles of Tax suspensions, Tax-LPs, and Tax-Se@LPs in rats following oral gavage are shown in Figure 5, with key parameters from a one-compartment model listed in Table 1. As presented in Figure 5, the plasma Tax concentrations for the liposomal groups were significantly higher than those for the Tax suspensions at all time points. The maximal concentration (C_{\max}) for Tax suspensions was 0.489 $\mu\text{g/mL}$, while it reached 0.608 $\mu\text{g/mL}$ for Tax-LPs and 0.599 $\mu\text{g/mL}$ for Tax-Se@LPs. This indicates that nanometerization promotes the oral absorption of Tax compared to conventional suspensions. Additionally, the peak time (T_{\max}) and half-life ($T_{1/2}$) of Tax were prolonged, likely due to the sustained release from liposomal preparations, which delays Tax metabolism after entering the circulation. The relative bioavailability of Tax-Se@LPs was calculated to be 216.65% compared with Tax suspensions, whereas it was merely 137.23% for Tax-LPs. Selenization reinforced the structural strength of liposomes, thus increasing the *in vivo* residence time due to enhanced stability.

Overall, plasma drug concentrations in rats were low due to the oxidation susceptibility of Tax,⁴⁰ with all formulations not exceeding 1 $\mu\text{g/mL}$. These findings align with Lakeev's study.⁴¹ Another report indicated that Tax was easily

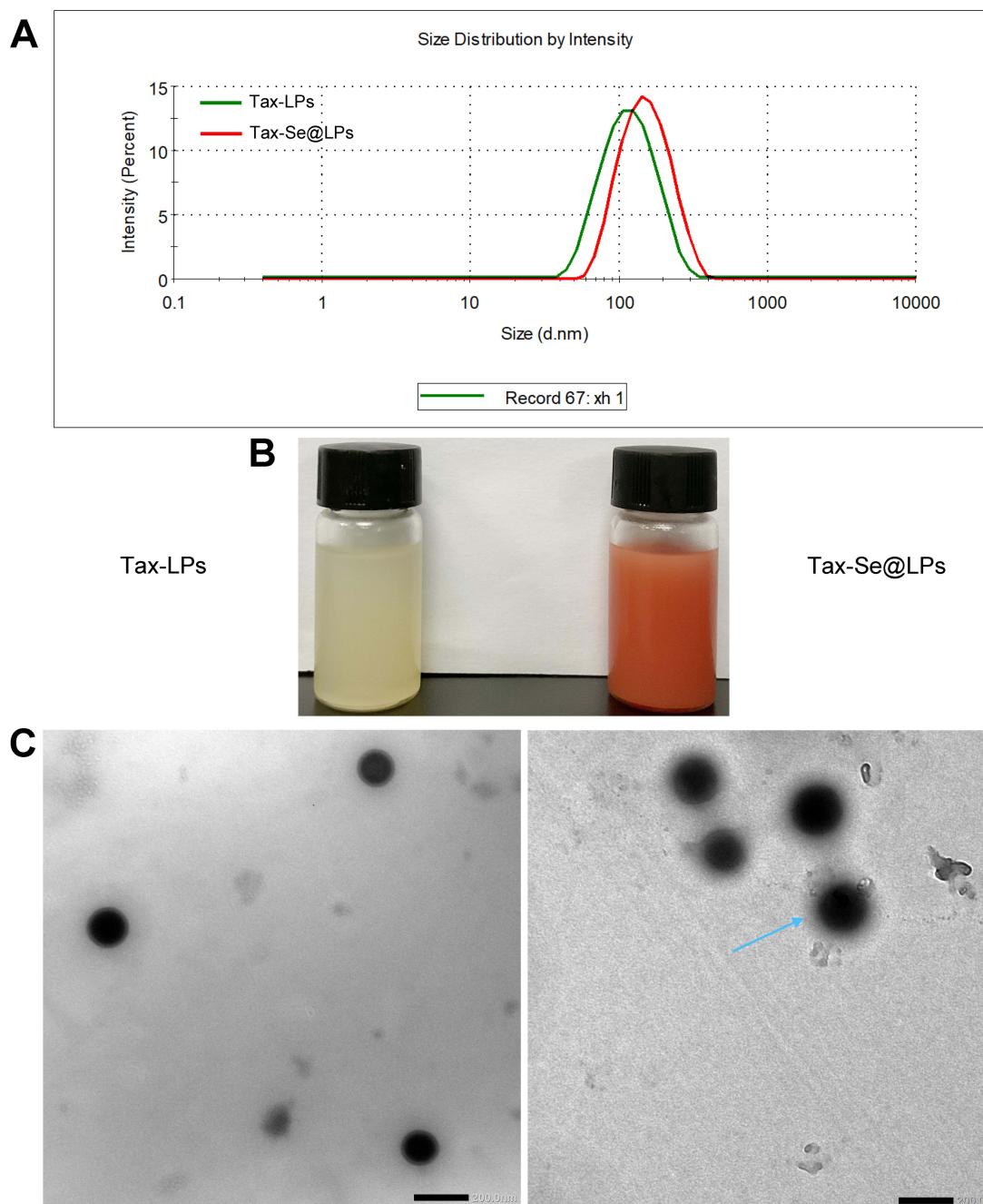


Figure 3 Particle size distribution (A), appearance (B), and micromorphology (C) of Tax-LPs and Tax-Se@LPs. The arrow denotes an increased electron-dense Corona as a result of selenization.

absorbed by the gastrointestinal tract, even in suspension form, and could be quickly eliminated from the body. Repeated Tax administration did not cause accumulation but affected the enzymatic system.⁴² More research on the pharmacokinetics of Tax, particularly regarding its nanomedicine applications, is limited. In our study, we first nanometerized Tax into liposomes for oral deliver to treat diabetes. The liposomal Tax, especially selenized liposomes, significantly extended its in vivo residence time, allowing Tax to exert its pharmacological effects effectively and placidly. The enhanced blood drug exposure and bioavailability of liposomal Tax surpass those of conventional formulations. This pharmacokinetic feature guarantees a desirable pharmacological effect during treatment.

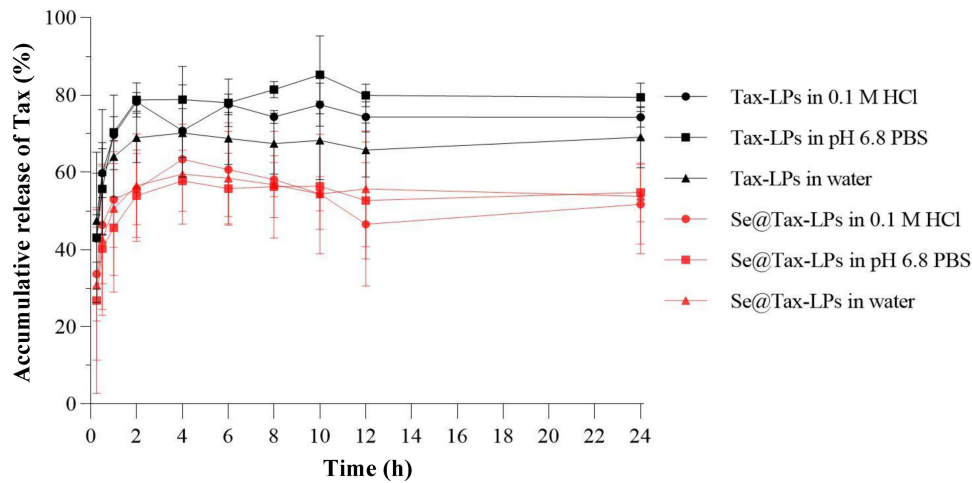


Figure 4 Drug release profiles of Tax-LPs and Tax-Se@LPs in the media of 0.1 M HCL, pH 6.8 PBS and deionized water.

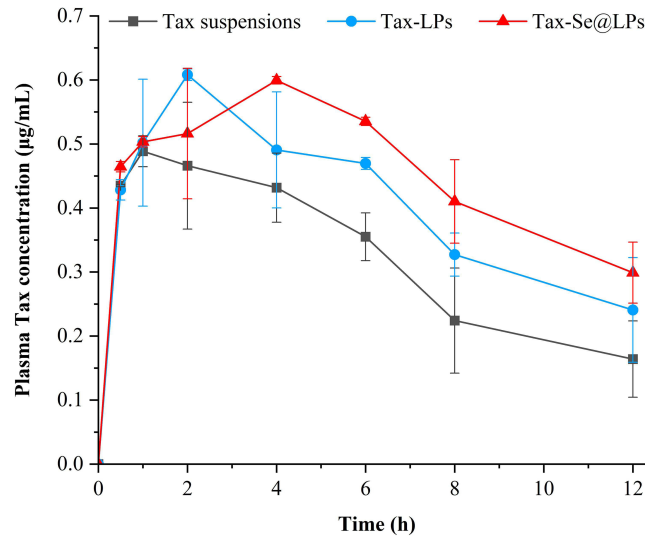


Figure 5 Blood drug concentration versus time profiles of Tax suspensions, Tax-LPs and Tax-Se@LPs in rats after oral administration.

Ameliorative Hypoglycemic Effect

The hypoglycemic effect of Tax-Se@LPs was compared to reference preparations. As shown in Figure 6, all GK rats kept up blood glucose concentrations above 12 mm before treatment, confirming their diabetic status. After administration, all

Table I Main Pharmacokinetic Parameters of Tax Observed in Rats After Oral Administration of Tax Suspensions, Tax-LPs and Tax-Se@LPs

Parameters	Tax Suspensions	Tax-LPs	Tax-Se@LPs
C_{max} (µg/mL)	0.514 ± 0.105	0.592 ± 0.088*	0.581 ± 0.161*
T_{max} (h)	1.200 ± 0.174	1.766 ± 0.213*	1.681 ± 0.315*
$T_{1/2}$ (h)	6.584 ± 0.632	7.578 ± 0.352*	13.114 ± 0.521**
$AUC_{0-\infty}$ (µg h/mL)	5.544 ± 0.343	7.608 ± 0.287*	12.011 ± 0.359**
RBA	/	137.23%	216.65%

Notes: One-way ANOVA, * $p < 0.05$, ** $p < 0.01$ compared with Tax suspensions.

Abbreviations: AUC, area under blood drug concentration–time curve; RBA, relative bioavailability.

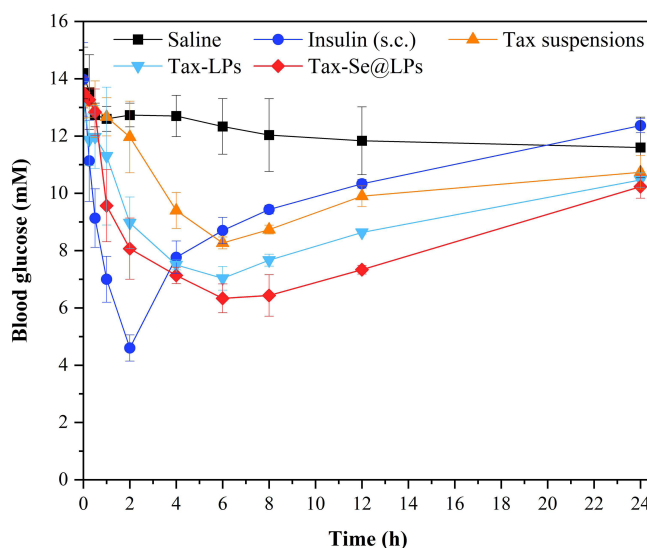


Figure 6 Curves of blood glucose concentration versus time following administration of saline, insulin (subcutaneous, s.c.), Tax suspensions, Tax-LPs and Tax-Se@LPs.

experimental rats experienced a decrease in blood glucose, though the extent varied among groups. Thereinto, the saline group exhibited only a slight decrease, primarily due to deprived food intake leading to natural glucose consumption. In contrast, the drug treatment groups showed significant reductions in blood glucose. Insulin injections (s.c.) resulted in a rapid decrease in blood glucose, but it rebounded quickly after 2 hours, indicating that while insulin has a strong hypoglycemic activity, it is not sustainable and may pose a risk of hypoglycemia.⁴³ Conversely, the hypoglycemic effects of Tax formulations were mild yet sustained. Tax suspensions also contributed to blood glucose reduction, attributed to its hypoglycemic and antioxidant properties,^{44,45} which alleviate oxidative stress in diabetic rats and enhance glucose consumption. The hypoglycemic effects of liposomal Tax were more pronounced and sustainable, maintaining blood glucose levels closer to physiological ranges for longer periods, thus reducing the risk of hypoglycemia and offering advantages in diabetes management. Compared with Tax-LPs, Tax-Se@LPs demonstrated even more significant hypoglycemic effects, due to the selenization of liposomes. Selenium, particularly in nano form, has inherent hypoglycemic properties.^{26,46,47} As combined with Tax, it produces a synergistic sensitization that ameliorates Tax's therapeutic efficacy.

GK rat is an early model of non-obese type 2 DM (T2DM).⁴⁸ These rats were inbred from Wistar rats without obesity but with insulin resistance after several generations of inbreeding. The metabolic and diabetic parameters of GK rats closely resemble those of human T2DM. Their blood glucose stability surpasses that of alloxan- and streptozotocin-induced diabetic rats. Consequently, GK rats are a widely used experimental model for T2DM. Additionally, GK rats exhibit reduced fasting blood glucose, with a more significant decrease observed when drug therapy is applied, allowing for the differentiation of pharmacodynamic effects among various formulations. Tax has been shown to regulate blood glucose by inhibiting α -glycosidase, α -amylase, and pancreatic lipase that reduces carbohydrates and lipid metabolism.^{49,50} In addition, Tax has a protective effect on the pancreas and liver through its antioxidant effects, which help alleviate insulin resistance.⁴⁴ These mechanisms contribute to Tax's effectiveness against diabetes. The hypoglycemic activity of Tax and its derivatives has been confirmed through in vitro and in vivo studies.^{8,9} However, the hypoglycemic effects were not remarkable due to the use of free or crude Tax, which has poor water solubility that limits its bioavailability. Our study first nanometerized Tax into liposomes followed by functionalization with selenium. This approach addresses the solubility and absorption issues of Tax while enhancing its therapeutic effect.

Cellular Uptake and Internalization Mechanisms

The cellular uptake of nanocarriers is typically assessed on enterocytes in vitro to predict in vivo absorption. Figure 7A shows the flow cytometric events of cellular uptake in Caco-2 cells for Tax-LPs and Tax-Se@LPs. Both nanocarriers demonstrated time-dependent cellular uptake. After 2 hours of incubation, the percentages of DiO-labeled Tax-LPs and

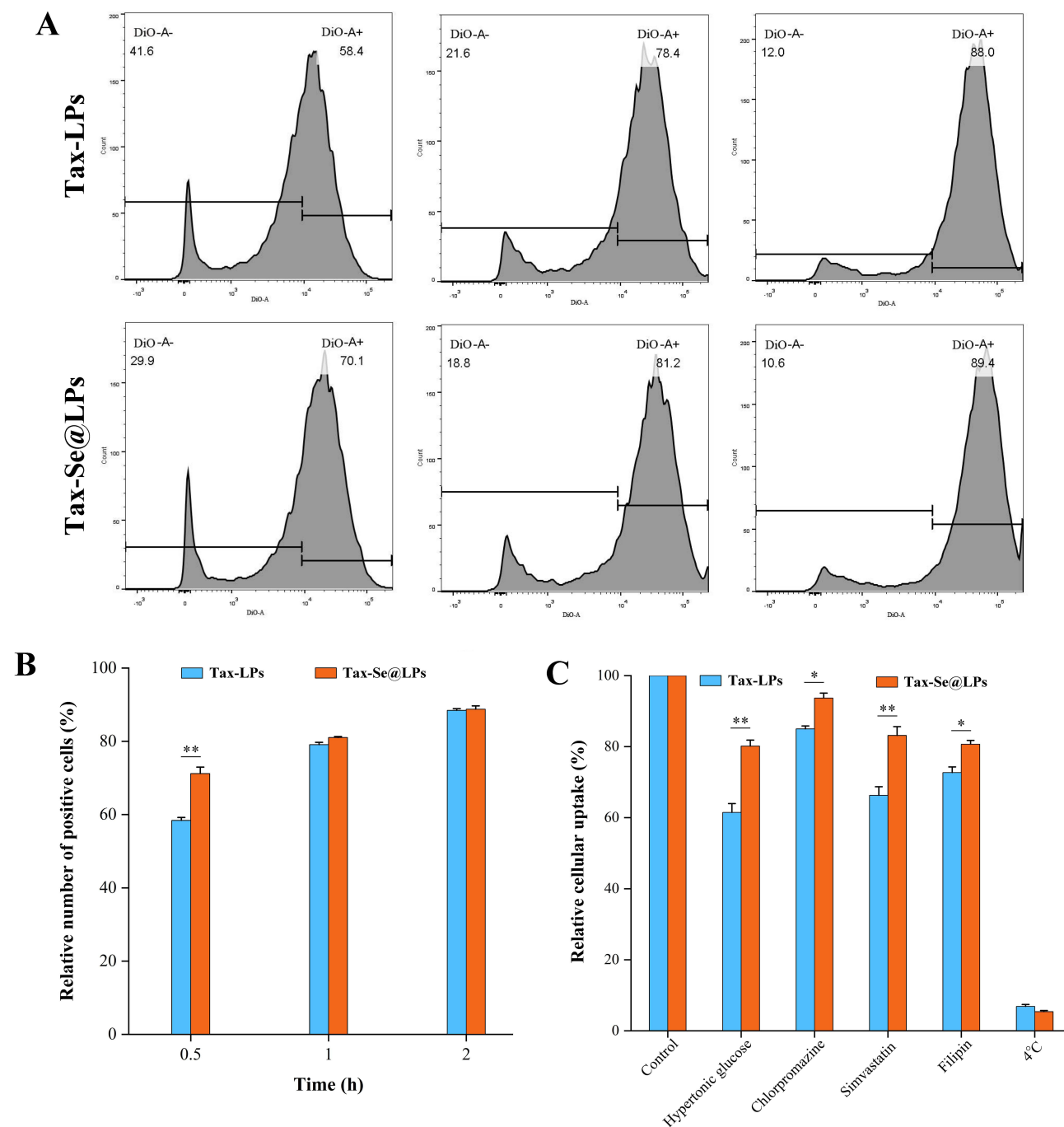


Figure 7 Cellular uptake of Tax-LPs and Tax-Se@LPs in Caco-2 cells assayed by flow cytometry: **(A)** the counts of positive cells stained by DiO-labeled nanovesicles; **(B)** statistical histograms of cellular uptake; and **(C)** relative cellular uptake in the presence of transport inhibitors or under 4°C. Paired t-test, ** $P < 0.01$, * $P < 0.05$, significantly different between two groups.

Tax-Se@LPs in positive cells were 88.0% and 89.4%, respectively (Figure 7B). Notably, the uptake of Tax-Se@LPs was slightly faster than that of Tax-LPs,^{27,51} likely due to enhance nonspecific phagocytosis, as selenized particulates tend to converge to the cell surface due to their higher density and lower net charge.^{52,53} Overall, the uptake trends for both nanovesicles are parallel, and selenization does not affect the transmembrane transport of vesicles. Nevertheless, Tax-LPs and Tax-Se@LPs shared different cellular trafficking mechanisms as shown in Figure 7C. The uptake rate of Tax-LPs was significantly reduced by hypertonic sucrose and simvastatin, both non-specific endocytosis inhibitors linked to clathrin and caveolin, as well as by Filipin, a specific caveolin-mediated endocytosis inhibitor. These findings indicate

that conventional liposomes can be efficiently internalized in Caco-2 cells through multiple pathways, highlighting their potential as oral drug delivery vehicles. In contrast, the uptake of Tax-Se@LPs was only moderately affected by hypertonic sucrose, simvastatin, and Filipin, suggesting a different uptake mechanism. While nonspecific clathrin- and caveolin-mediated endocytosis primarily drive the uptake of Tax-LPs, Tax-Se@LPs rely on nonspecific clathrin-mediated endocytosis and caveolin-mediated endocytosis. This reveals that selenization alters the cellular uptake mechanisms of liposomes. In addition, both nanocarriers' uptake was strikingly inhibited at 4°C, as cytosol (membrane transport) is energy-dependent under 4°C. As known, the process of cytosol (membrane mobile transport) is energy-dependent.⁵⁴ The reduced cellular uptake at low temperatures indicates that nanovesicles are internalized mainly via cytosol rather than passive transport, though other transport patterns, including transporter-mediated uptake, cannot be excluded. Although the specific transporters responsible for the transport of Tax-Se@LPs remain unidentified, the active transport mode of Tax-Se@LPs facilitates their better absorption by the intestinal epithelia.

The cell affinity of nanocarriers, such as liposomes and lipid nanoparticles, can indeed be assessed through cellular internalization using CLSM imaging. Our study observed that after co-incubation for 0.5 hours, both types of nanovesicles exhibited noticeable fluorescence, with Tax-Se@LPs demonstrating a slightly higher fluorescence intensity compared to Tri-LPs (Figure 8). This observation aligns with the finding related to cellular uptake at 0.5 h, suggesting that selenized liposomes are more readily internalized by the absorptive cells, potentially enhancing their oral bioavailability. Moreover, CLSM images indicated that the fluorescence associated with the nanovesicles was distributed throughout the cell rather than being confined to the cytoplasm. This distribution may be attributed to the reinforced stability of selenized liposomes, which helps facilitate their escape from lysosomes.⁵⁵ As a result, this enables the translocation of nanomedicine from the apical membrane of the intestinal epithelium to the basolateral side, thereby improving overall absorption through integral nanovesicles. This mechanism is critical for enhancing the bioavailability and therapeutic efficacy of the delivered phytomedicine.

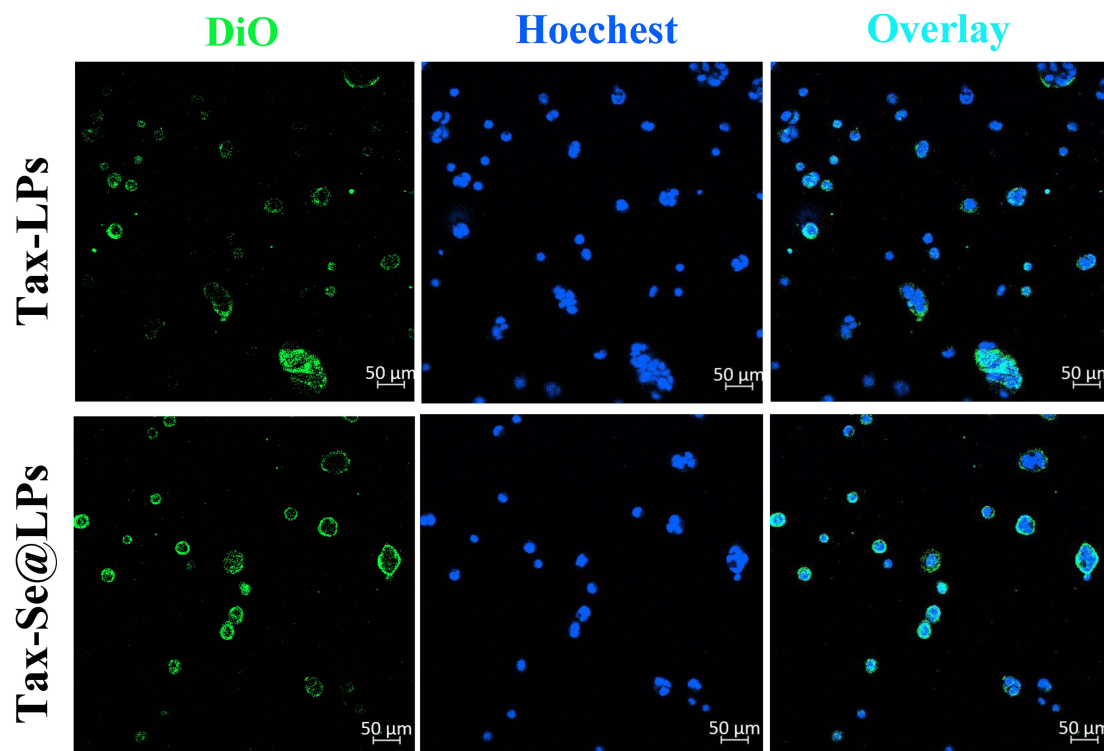


Figure 8 Cellular internalization of Tax-LPs and Tax-Se@LPs observed by confocal laser scanning microscopy (CLSM).

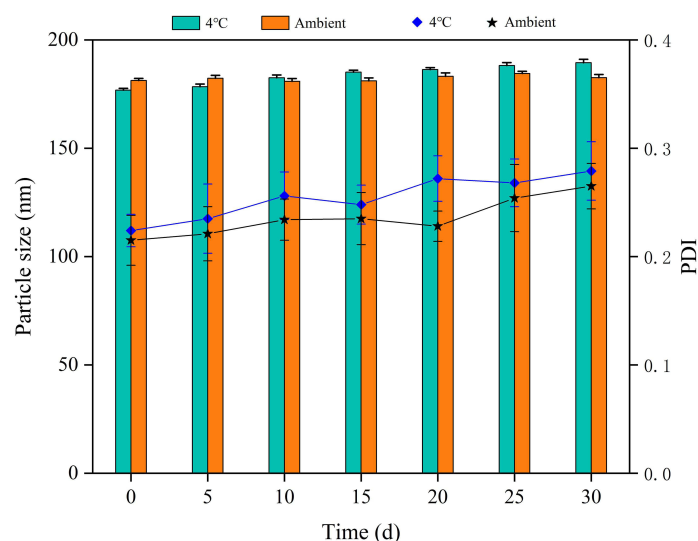


Figure 9 In vitro stability of Tax-Se@LPs assessed through particle size and polydispersity (PDI) during storing at 4°C and ambient conditions.

Reinforced in vitro/vivo Stability via Selenization

Changes in particle size and PDI reflect the in vitro stability of nanovehicles during storage. Figure 9 shows the evolutions of these parameters for Tax-Se@LPs. Both particle size and PDI exhibited only marginal changes at 4°C and ambient conditions over time; however, the PDI increased slightly yet remained below 0.3. This minor increase indicates some particle aggregation within the colloidal system, a common phenomenon in thermodynamically unstable systems.^{56,57} Overall, Tax-Se@LPs demonstrate kinetic stability; nonetheless, lyophilization is required for this nano-medicine to facilitate the bench-to-clinic translation in the future.

The changes in particle size, PDI, and ζ potential of Tax-LPs and Tax-Se@LPs in various biorelevant media over time are shown in Figure 10. In deionized water, both formulations exhibited minimal changes in these stability indicators over 8 hours, indicating their physical stability. In the medium of SGF, both Tax-LPs and Tax-Se@LPs exhibited an increase in particle size and PDI over time, with a significant in ζ potential, especially for Tax-LPs. Tax-LPs became positively charged, while Tax-Se@LPs' ζ potential transitioned from negative to positive. The lower pH and higher ionic strength of SGF likely reversed the surface charge of Tax-LPs, as hydrogen ions interacted with the negative surface, resulting in their protonation. This protonation reduced the absolute surface potential,^{58,59} hence the increase of PDI, due to potential particle aggregation. Tax-LPs showed greater variability in particle size compared to Tax-Se@LPs in SGF, manifesting that the selenized nanovesicles were more stable in SIF, Tax-LPs also experienced an increase in particle size and PDI alongside a slight decrease in the absolute potential, indicating partial protonation, though this effect was less pronounced due to a higher pH. Conversely, the protonation effect on Tax-Se@LPs in SIF was marginal. Overall, Tax-Se@LPs demonstrated high gastrointestinal stability, attributed to the surface selenization that enhances the structural stability of nanovesicles.

Conclusions

Diabetes mellitus poses significant health risks and presents complex treatment challenges. This work explores the preparation and characteristics of taxifolin-loaded selenized liposomes (Tax-Se@LPs) in a diabetic model. Through film hydration and in situ reduction techniques, we optimized formulation parameters such as the phospholipid/cholesterol and drug/lipid ratios, resulting in stable nanoliposomes. In vitro release experiments revealed a delayed drug release rate for Tax-Se@LPs, which helps ameliorate oral bioavailability. Pharmacokinetic studies showed a significant enhancement in the relative bioavailability in terms of Tax-Se@LPs in rats, reaching 216.65%. Furthermore, Tax-Se@LPs exhibited a prolonged hypoglycemic effect in the GK rat model, outperforming other formulations. Their cellular uptake mechanism differed from conventional liposomes while maintaining similar internalization capacity. In addition, Tax-Se@LPs exhibited favorable stability during storage, suggesting potential for diabetes management. It is important to acknowledge the inherent limitations of the GK diabetic

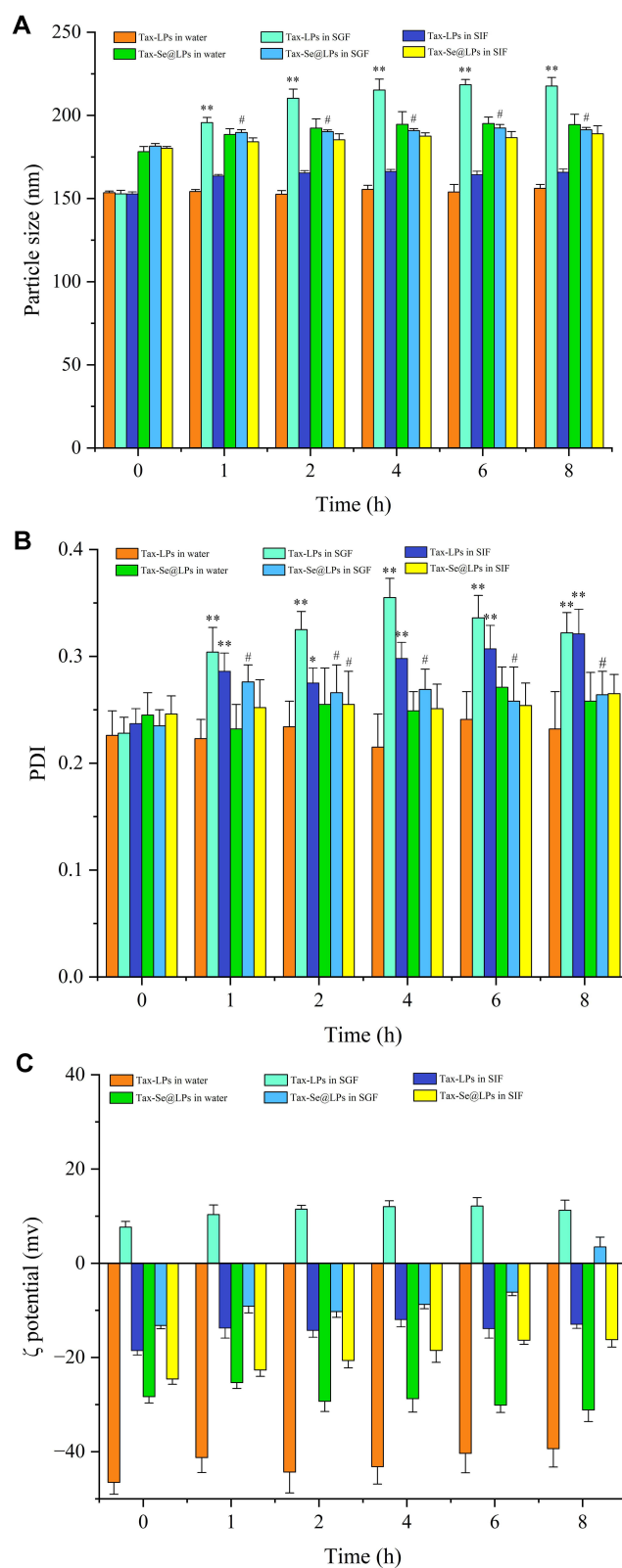


Figure 10 In vivo stability of Tax-LPs and Tax-Se@LPs tested in various biorelevant media over time through particle size (A), PDI (B), and ζ potential (C). Paired t-test, $**P < 0.01$, $*P < 0.05$, significantly different compared to the initial time point (0 h) for Tax-LPs; $###P < 0.01$, $##P < 0.05$, significantly different compared to the initial time point (0 h) for Tax-Se@LPs.

model. To enhance the clinical relevance and translational value of future research, it would be advantageous to employ animal models that more accurately replicate the pathophysiological progression and clinical manifestations of human diabetes.

Acknowledgment

This work was jointly supported by the Projects of Construction and Practice of PDCA Closed-loop Management Internal Control System for Biosafety of Laboratory Animals in Universities (21SYB08), Agricultural Research and Technology Promotion Demonstration Projects of the Department of Agriculture and Rural Development in Guangdong Province in 2024 (2023-440000-58010200-9645), Guangdong Basic and Applied Basic Research Foundation (2023A1515012326), and Funding by Science and Technology Projects in Guangzhou (202201010018).

Disclosure

The authors report no conflicts of interest in this work.

References

1. Balooch Hasankhani M, Mirzaei H, Karamoozian A. Global trend analysis of diabetes mellitus incidence, mortality, and mortality-to-incidence ratio from 1990 to 2019. *Sci Rep*. 2023;13(1):21908. doi:10.1038/s41598-023-49249-0
2. Mishra V, Nayak P, Sharma M, et al. Emerging treatment strategies for diabetes mellitus and associated complications: an update. *Pharmaceutics*. 2021;13(10):1568. doi:10.3390/pharmaceutics13101568
3. Ren Y, Nie L, Zhu S, et al. Nanovesicles-mediated drug delivery for oral bioavailability enhancement. *Int J Nanomed*. 2022;17:4861–4877. doi:10.2147/IJN.S382192
4. Ruan S, Guo X, Ren Y, et al. Nanomedicines based on trace elements for intervention of diabetes mellitus. *Biomed Pharmacother*. 2023;168:115684. doi:10.1016/j.biopha.2023.115684
5. Jadhav S, Yadav A. Phytoconstituents based nanomedicines for the management of diabetes: a review. *Pharm Nanotechnol*. 2023;11(3):217–237. doi:10.2174/2211738511666230118095936
6. Anthony KP, Saleh MA. Free radical scavenging and antioxidant activities of silymarin components. *Antioxidants*. 2013;2(4):398–407. doi:10.3390/antiox2040398
7. Sunil C, Xu B. An insight into the health-promoting effects of taxifolin (dihydroquercetin). *Phytochemistry*. 2019;166:112066. doi:10.1016/j.phytochem.2019.112066
8. Yoon KD, Lee JY, Kim TY, et al. In vitro and in vivo anti-hyperglycemic activities of taxifolin and its derivatives isolated from pigmented rice (*Oryza sativa* L. cv. *Superhongmi*). *J Agric Food Chem*. 2020;68(3):742–750. doi:10.1021/acs.jafc.9b04962
9. Kondo S, Adachi SI, Yoshizawa F, et al. Antidiabetic effect of taxifolin in cultured l6 myotubes and type 2 diabetic model KK-A(y)/Ta mice with hyperglycemia and hyperuricemia. *Curr Issues mol Biol*. 2021;43(3):1293–1306. doi:10.3390/cimb43030092
10. Porter CJH, Trevaskis NL, Charman WN. Lipids and lipid-based formulations: optimizing the oral delivery of lipophilic drugs. *Nat Rev Drug Discov*. 2007;6(3):231–248. doi:10.1038/nrd2197
11. Xing H, Wang H, Wu B, et al. Lipid nanoparticles for the delivery of active natural medicines. *Curr Pharm Des*. 2017;23(43):6705–6713. doi:10.2174/1381612824666171128105853
12. Zhang A, Li J, Wang S, et al. Rapid and improved oral absorption of N-butylphthalide by sodium cholate-appended liposomes for efficient ischemic stroke therapy. *Drug Deliv*. 2021;28(1):2469–2479. doi:10.1080/10717544.2021.2000678
13. Nora GI, Venkatasubramanian R, Strindberg S, et al. Combining lipid based drug delivery and amorphous solid dispersions for improved oral drug absorption of a poorly water-soluble drug. *J Control Release*. 2022;349:206–212. doi:10.1016/j.jconrel.2022.06.057
14. Liang D, Liu C, Li J, et al. Engineering probiotics-derived membrane vesicles for encapsulating fucoxanthin: evaluation of stability, bioavailability, and biosafety. *Food Funct*. 2023;14(8):3475–3487. doi:10.1039/d2fo04116b
15. Liu F, Meng F, Yang Z, et al. Exosome-biomimetic nanocarriers for oral drug delivery. *Chin Chem Lett*. 2024;35(9):109335. doi:10.1016/j.cclet.2023.109335
16. Lee MK. Liposomes for enhanced bioavailability of water-insoluble drugs: in vivo evidence and recent approaches. *Pharmaceutics*. 2020;12(3):264. doi:10.3390/pharmaceutics12030264
17. Zhang X, Chen G, Zhang T, et al. Effects of PEGylated lipid nanoparticles on the oral absorption of one BCS II drug: a mechanistic investigation. *Int J Nanomed*. 2014;9:5503–5514. doi:10.2147/ijn.s73340
18. Yamazoe E, Fang JY, Tahara K. Oral mucus-penetrating PEGylated liposomes to improve drug absorption: differences in the interaction mechanisms of a mucoadhesive liposome. *Int J Pharm*. 2021;593:120148. doi:10.1016/j.ijpharm.2020.120148
19. Zhao Y, Yin W, Yang Z, et al. Nanotechnology-enabled M2 macrophage polarization and ferroptosis inhibition for targeted inflammatory bowel disease treatment. *J Control Release*. 2024;367:339–353. doi:10.1016/j.jconrel.2024.01.051
20. Zhu MJ, Zhu SP, Liu QB, et al. Selenized liposomes with ameliorative stability that achieve sustained release of emodin but fail in bioavailability. *Chin Chem Lett*. 2023;34(1):107482. doi:10.1016/j.cclet.2022.04.080
21. Battogtokh G, Joo Y, Abuzar SM, et al. Gelatin coating for the improvement of stability and cell uptake of hydrophobic drug-containing liposomes. *Molecules*. 2022;27(3):1041. doi:10.3390/molecules27031041
22. Paserin D, Ghizdareanu AI, Enascuta CE, et al. Coating materials to increase the stability of liposomes. *Polymers*. 2023;15(3):782. doi:10.3390/polym15030782
23. Beketov AA, Mikhailov IV, Darinskii AA. Stability of DMPC liposomes externally conjugated with branched polyglycerol. *Int J mol Sci*. 2022;23(16):9142. doi:10.3390/ijms23169142

24. Cao Y, Dong X, Chen X. Polymer-modified liposomes for drug delivery: from fundamentals to applications. *Pharmaceutics*. 2022;14(4):778. doi:10.3390/pharmaceutics14040778
25. Xie Q, Deng W, Yuan X, et al. Selenium-functionalized liposomes for systemic delivery of doxorubicin with enhanced pharmacokinetics and anticancer effect. *Eur J Pharm Biopharm*. 2018;122:87–95. doi:10.1016/j.ejpb.2017.10.010
26. Deng W, Wang H, Wu B, et al. Selenium-layered nanoparticles serving for oral delivery of phytomedicines with hypoglycemic activity to synergistically potentiate the antidiabetic effect. *Acta Pharm Sin B*. 2019;9(1):74–86. doi:10.1016/j.apsb.2018.09.009
27. Ren Y, Qi C, Ruan S, et al. Selenized polymer-lipid hybrid nanoparticles for oral delivery of tripterine with ameliorative oral anti-enteritis activity and bioavailability. *Pharmaceutics*. 2023;15(3):821. doi:10.3390/pharmaceutics15030821
28. Xu K, Huang P, Wu Y, et al. Engineered selenium/human serum albumin nanoparticles for efficient targeted treatment of Parkinson's disease via oral gavage. *ACS Nano*. 2023;17(20):19961–19980. doi:10.1021/acsnano.3c05011
29. Xuan G, Zhang M, Chen Y, et al. Design and characterization of a cancer-targeted drug co-delivery system composed of liposomes and selenium nanoparticles. *J Nanosci Nanotechnol*. 2020;20(9):5295–5304. doi:10.1166/jnn.2020.17882
30. Liu S, Chen Q, Yan L, et al. Phytosomal tripterine with selenium modification attenuates the cytotoxicity and restrains the inflammatory evolution via inhibiting NLRP3 inflammasome activation and pyroptosis. *Int Immunopharmacol*. 2022;108:108871. doi:10.1016/j.intimp.2022.108871
31. Ye D, Ding D, Pan LY, et al. Natural coptidis rhizoma nanoparticles improved the oral delivery of docetaxel. *Int J Nanomed*. 2024;19:8417–8436. doi:10.2147/ijn.S470853
32. Islam J, Shree A, Vafa A, et al. Taxifolin ameliorates Benzo[a]pyrene-induced lung injury possibly via stimulating the Nrf2 signalling pathway. *Int Immunopharmacol*. 2021;96:107566. doi:10.1016/j.intimp.2021.107566
33. Yang CJ, Wang ZB, Mi YY, et al. UHPLC-MS/MS determination, pharmacokinetic, and bioavailability study of taxifolin in rat plasma after oral administration of its nanodispersion. *Molecules*. 2016;21(4):494. doi:10.3390/molecules21040494
34. Khalid MF, Akash MSH, Rehman K, et al. Modulation of metabolic pathways and protection against cadmium-induced disruptions with taxifolin-enriched extract. *ACS Omega*. 2024;9(3):4057–4072. doi:10.1021/acsomega.3c08989
35. Wang J, Pan H, Li J, et al. Cell membrane-coated mesoporous silica nanorods overcome sequential drug delivery barriers against colorectal cancer. *Chin Chem Lett*. 2023;34(6):107828. doi:10.1016/j.ccl.2022.107828
36. Agmo Hernández V. An overview of surface forces and the DLVO theory. *ChemTexts*. 2023;9(4):10. doi:10.1007/s40828-023-00182-9
37. Bhattacharjee S. Understanding the burst release phenomenon: toward designing effective nanoparticulate drug-delivery systems. *Ther Deliv*. 2021;12(1):21–36. doi:10.4155/tde-2020-0099
38. Zhao P, Xia X, Xu X, et al. Nanoparticle-assembled bioadhesive coacervate coating with prolonged gastrointestinal retention for inflammatory bowel disease therapy. *Nat Commun*. 2021;12(1):7162. doi:10.1038/s41467-021-27463-6
39. Ren Y, Wu W, Zhang X. The feasibility of oral targeted drug delivery: gut immune to particulates? *Acta Pharm Sin B*. 2023;13(6):2544–2558. doi:10.1016/j.apsb.2022.10.020
40. Bruić M, Pirković A, Borozan S, et al. Antioxidative and anti-inflammatory effects of taxifolin in H(2)O(2)-induced oxidative stress in HTR-8/SVneo trophoblast cell line. *Reprod Toxicol*. 2024;126:108585. doi:10.1016/j.reprotox.2024.108585
41. Lakeev AP, Yanovskaya EA, Yanovsky VA, et al. Novel aspects of taxifolin pharmacokinetics: dose proportionality, cumulative effect, metabolism, microemulsion dosage forms. *J Pharm Biomed Anal*. 2023;236:115744. doi:10.1016/j.jpba.2023.115744
42. Yanovskaya EA, Frelikh GA, Lakeev AP, et al. Pharmacokinetics of dihydroquercetin after single and repeated administration to rats. *Bull Exp Biol Med*. 2024;176(6):743–746. doi:10.1007/s10517-024-06100-4
43. Kang H, Meng F, Liu F, et al. Nanomedicines targeting ferroptosis to treat stress-related diseases. *Int J Nanomed*. 2024;19:8189–8210. doi:10.2147/ijn.S476948
44. Taldaev A, Savina AD, Olicheva VV, et al. Protective properties of spheroidal taxifolin form in streptozotocin-induced diabetic rats. *Int J mol Sci*. 2023;24(15):11962. doi:10.3390/ijms241511962
45. Shubina VS, Kozina VI, Shatalin YV. Comparison of antioxidant properties of a conjugate of taxifolin with glyoxylic acid and selected flavonoids. *Antioxidants*. 2021;10(8):1262. doi:10.3390/antiox10081262
46. Al-Quraishy S, Dkhil MA, Abdel Moneim AE. Anti-hyperglycemic activity of selenium nanoparticles in streptozotocin-induced diabetic rats. *Int J Nanomed*. 2015;10:6741–6756. doi:10.2147/IJN.S91377
47. Deng W, Xie Q, Wang H, et al. Selenium nanoparticles as versatile carriers for oral delivery of insulin: insight into the synergic antidiabetic effect and mechanism. *Nanomedicine*. 2017;13(6):1965–1974. doi:10.1016/j.nano.2017.05.002
48. Al-Awar A, Kupai K, Veszelka M, et al. Experimental diabetes mellitus in different animal models. *J Diabetes Res*. 2016;2016:9051426. doi:10.1155/2016/9051426
49. Su H, Ruan YT, Li Y, et al. In vitro and in vivo inhibitory activity of taxifolin on three digestive enzymes. *Int J Biol Macromol*. 2020;150:31–37. doi:10.1016/j.ijbiomac.2020.02.027
50. Rehman K, Chohan TA, Waheed I, et al. Taxifolin prevents postprandial hyperglycemia by regulating the activity of α -amylase: evidence from an in vivo and in silico studies. *J Cell Biochem*. 2019;120(1):425–438. doi:10.1002/jcb.27398
51. Yin J, Hou Y, Yin Y, et al. Selenium-coated nanostructured lipid carriers used for oral delivery of berberine to accomplish a synergic hypoglycemic effect. *Int J Nanomed*. 2017;12:8671–8680. doi:10.2147/IJN.S144615
52. Yazdimamaghani M, Barber ZB, Hadipour Moghaddam SP, et al. Influence of silica nanoparticle density and flow conditions on sedimentation, cell uptake, and cytotoxicity. *Mol Pharm*. 2018;15(6):2372–2383. doi:10.1021/acs.molpharmaceut.8b00213
53. Metwally S, Stachewicz U. Surface potential and charges impact on cell responses on biomaterials interfaces for medical applications. *Mater Sci Eng C*. 2019;104:109883. doi:10.1016/j.msec.2019.109883
54. Dos Santos T, Varela J, Lynch I, et al. Effects of transport inhibitors on the cellular uptake of carboxylated polystyrene nanoparticles in different cell lines. *PLoS One*. 2011;6(9):e24438. doi:10.1371/journal.pone.0024438
55. Li Y, Cheng Q, Jiang Q, et al. Enhanced endosomal/lysosomal escape by distearoyl phosphoethanolamine-polycarboxybetaine lipid for systemic delivery of siRNA. *J Control Release*. 2014;176:104–114. doi:10.1016/j.jconrel.2013.12.007
56. Zhang W. Nanoparticle aggregation: principles and modeling. *Adv Exp Med Biol*. 2014;811:19–43. doi:10.1007/978-94-017-8739-0_2
57. Li H, Wang X, Qiao D, et al. Mechanism of nanoparticle aggregation in gas-liquid microfluidic mixing. *Chin Chem Lett*. 2024;35(4):108747. doi:10.1016/j.ccl.2023.108747

58. Carrasco MJ, Alishetty S, Alameh MG, et al. Ionization and structural properties of mRNA lipid nanoparticles influence expression in intramuscular and intravascular administration. *Commun Biol.* **2021**;4(1):956. doi:10.1038/s42003-021-02441-2
59. Athavale R, Sapre N, Rale V, et al. Tuning the surface charge properties of chitosan nanoparticles. *Mater Lett.* **2022**;308:131114. doi:10.1016/j.matlet.2021.131114

International Journal of Nanomedicine

Publish your work in this journal

The International Journal of Nanomedicine is an international, peer-reviewed journal focusing on the application of nanotechnology in diagnostics, therapeutics, and drug delivery systems throughout the biomedical field. This journal is indexed on PubMed Central, MedLine, CAS, SciSearch®, Current Contents®/Clinical Medicine, Journal Citation Reports/Science Edition, EMBase, Scopus and the Elsevier Bibliographic databases. The manuscript management system is completely online and includes a very quick and fair peer-review system, which is all easy to use. Visit <http://www.dovepress.com/testimonials.php> to read real quotes from published authors.

Submit your manuscript here: <https://www.dovepress.com/international-journal-of-nanomedicine-journal>

Dovepress
Taylor & Francis Group